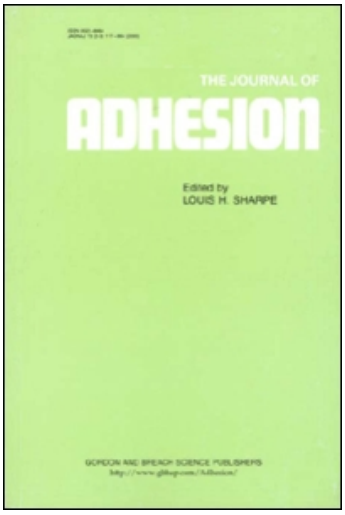

The Journal of Adhesion
Publication details, including instructions for authors and subscription information:
http://www.informaworld.com/smpp/title~content=t713453635

Time and Size Correlations of Photon and Radiowave Bursts from Peeling Pressure Sensitive Adhesives in Air

E. E. Donaldson[a]; J. T. Dickinson[a]; X. A. Shen[a]
[a] Department of Physics, Washington State University, Pullman, WA, U.S.A.

To cite this Article Donaldson, E. E. , Dickinson, J. T. and Shen, X. A.(1986) 'Time and Size Correlations of Photon and Radiowave Bursts from Peeling Pressure Sensitive Adhesives in Air', The Journal of Adhesion, 19: 3, 267 — 286
To link to this Article: DOI: 10.1080/00218468608071228
URL: http://dx.doi.org/10.1080/00218468608071228

J. Adhesion, 1986, Vol. 19, pp. 267–286
0021-8464/86/1904–0267 $18.50/0

Printed in the United Kingdom

Time and Size Correlations of Photon and Radiowave Bursts from Peeling Pressure Sensitive Adhesives in Air

E. E. DONALDSON, J. T. DICKINSON, and X. A. SHEN

Department of Physics, Washington State University, Pullman, WA 99164-2814, U.S.A.

(*Received June* 10, 1985; *in final form October* 15, 1985)

During separation in air of an adhesive from a polymer substrate we have observed intense *bursts* of photons (phE for photon emission) and long wavelength electromagnetic radiation (RE-for radiowave emission), similar to those reported earlier by Deryagin *et al.* In this paper we present detailed measurements of phE time distributions as well as time and size correlations between bursts of phE and RE. These results support the view that patches of electrical charge produced by charge separation between dissimilar materials lead to gaseous breakdown in and near the crack tip. We discuss the role of these discharges in producing sustained phE *after* the discharge has been extinguished.

KEY WORDS Fracture; Adhesive Failure; Fracto-Emission; Triboluminescence; Electromagnetic Radiation; Electrical Charge Separation.

1 INTRODUCTION

The emission of a wide variety of particles and radiation has been observed accompanying the fracture of a number of materials.[1–14] The range of materials from which such emission has been detected include crystalline materials such as alkali halides and metal oxides, polymers and composites, as well as several interfaces, including those involving adhesives. The types of emission observed include

electrons, positive ions, neutral atoms and molecules, and radiation consisting of visible photons (phE) and long wavelength electromagnetic radiation [radio emission (RE)]. The collective term describing all of these emissions is "fractoemission" because fracture appears to be a necessary prerequisite for its occurrence.

We have recently presented a model[11–14] which explains the intense long lasting electron, positive ion, and photon emission observed during adhesive failure. The sequence of events producing this intense emission is initiated or triggered by the electrical charge separation which is produced when fracture occurs between dissimilar materials. This separation of charge results in discharges in the vicinity of the detachment line or crack tip. These discharges cause excitation of the newly created fracture surfaces as well as any gases present. The microdischarges themselves produce phE and RE directly. In addition, these discharges lead to particle bombardment of the newly created fracture surfaces, thereby exciting them. The deexcitation of these surfaces *via* thermally stimulated relaxation leads to sustained emission following the discharge.

The production of radiation during the failure of an adhesive joint has been previously observed. Deryagin[15] and co-workers reported that such failure produces light and radio frequency radiation in the form of bursts. They showed that these bursts were produced simultaneously and have the same duration (about 10^{-3} to 10^{-4} s).

Deryagin, Skinner,[16] and Huntberger[17] have examined the role of electrostatic forces as part of the work of adhesion. Clearly these forces exist and may be perceptible in some cases; however, Huntsberger[17] concludes that electrostatic contributions to adhesion will generally be negligible.

In this work we examine the peeling of a common pressure sensitive adhesive, focusing on a detailed characterization of the time distributions of the phE bursts as well as the time and intensity correlations of the phE and RE bursts. We also propose more detailed phE (or triboluminescence) mechanisms in light of these results.

These experiments were conducted in air at 22 ± 2 C; similar experiments carried out in vacuum are in progress. Working in air we are limited to the detection of two kinds of fractoemission; namely, phE and RE, which have detectors operable in air. There

are several distinct advantages of conducting experiments in air: pump down delays are eliminated; it is easier to refrigerate the PMT and decrease dramatically its background count rate; and the mechanical apparatus was simpler to operate in air. Finally, most practical fracture problems are encountered in air so that any improved knowledge of fracture in air could be used in applications more readily.

The charge separation which leads to microdischarges and fractoemission may arise in a range of situations including adhesive failure and the breaking of chemical bonds. In addition to possible applications to the investigation of failure mechanisms of adhesives, these studies of fractoemission in air may also be applicable to the production and processing of pressure sensitive adhesives as well as to a variety of tribology problems in which surface charges are produced.

2 EXPERIMENTAL

We selected 3 M Scotch Brand Filament Tape No. 893 as a test material. The adhesive is a natural rubber combined with varying amounts of a tackifying agent which is a hydrocarbon resin appearing to be terpene based. More tackifier is used on the face of the adhesive and less in the saturating layer binding the filaments to the backing. The polyester tape backing has been treated with a release coating with a critical surface tension for wetting of approximately 21 dyne/cm. The advantages of this choice of material were its availability, the reproducibility of results in air, and its tendency to produce copious emission. Similar tests on other adhesive-polymer systems showed that a number of these observations were also applicable to a wide range of materials.

The geometry of the peeling and detectors is shown in Figure 1. The loading was basically that of a T-peel test. Samples were composed of multiple layers of tape and separated on the axis by the two spools. The samples were arranged so that separation could be produced either between the isoprene-based adhesive layers of two tapes or between the adhesive of one tape and the release-coated polyester backing of a second tape. A third failure mode involved the delamination of the glass filament layer from the

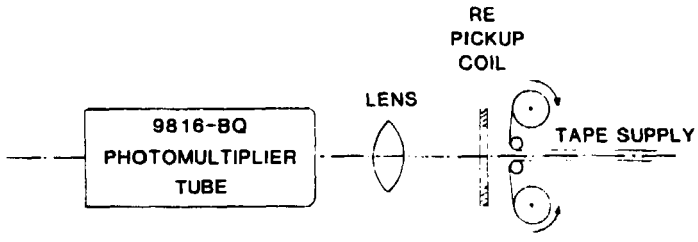

FIGURE 1 Schematic diagram of the experiment.

backing of a single layer of tape. During delamination, the filaments appeared to separate cleanly from the inner filament-saturating adhesive layer and this produced emission characteristic of the glass filament-adhesive interface.

The peel forces for this tape were measured in a T-peel configuration at a laboratory temperature of 22 C. The average peel force was lowest at slow peel speeds (<1 mm/s) and higher at greater peel speeds (3 cm/s). For the three tape assemblies just described, the ranges of peel force were:

Two Adhesive Layers Together,	310–480 grams (weight)/cm;
One Layer on Coated Backing,	50–240 grams (weight)/cm;
Delamination of Filaments,	240–470 grams (weight)/cm.

For detection of RE, a flat coil with an inductance of 0.77 mH was placed several cm in front of the tape separation zone (see Figure 1). Electrical discharges in the vicinity of the coil are like rapidly oscillating charged particles, which produce radiation. Because of our proximity to the source, the coil is sensitive to the changing B field of what is known as the *near field.* The response of the coil circuit to this stimulation is an oscillation at a characteristic frequency of 400 KHz. These oscillations are damped in time with an initial amplitude of 1 to 10 mV with the largest lasting for nearly 100 μs. We refer to these ring-down oscillations as *RE bursts,* realizing that the actual electromagnetic pulse is much shorter.

The RE bursts were amplified by a wide band differential amplifier with low noise and high gain. The amplified signal then entered a discriminator which produced a clean pulse every time an

oscillation occurred above the discriminator threshold, usually set just above the noise. These pulses could then be counted; large amplitude RE bursts produced more counts. It was also possible to derive a single pulse at the instant of the initial rise of each RE burst. These single pulses could be used to count the number of RE bursts or to trigger various circuits. The ringing of the RE bursts necessitated a 100 μs dead time between detection of individual successive bursts.

A quartz lens gathered light to the central region of the photomultiplier tube [EMI 9816BQ], which was operated at -40 C to reduce the background or dark count rate. The PMT had a quantum efficiency of approximately 10 percent so the overall detection efficiency for photons coming from the peel region was approximately 10^{-2}. The background was 10 counts/s with all light leaks eliminated.

The thermoelectric refrigerator and PMT housing was provided with an integral amplifier-discriminator which shaped the PMT pulses into 2V pulses about 0.07 μs wide. At low instantaneous levels of phE, pulses from the PMT and its integral amplifier-discriminator could be used directly in a pulse counting mode. Thus, these pulses were fed into a multichannel scaler which provided a direct measure of counts *vs* time. When the count rate exceeded 10^7 counts/s, the amplifier-discriminator overloaded and an analog current measurement was used. In this technique the PMT output for a large burst of photons was treated like a rapidly changing DC current. After converting this current to a voltage (by passing it through a resistor), the resulting signal could be amplified by a fast DC amplifier [EGG Ortec 579, <5 ns rise time]. This amplified signal was then digitized at time intervals of 50–100 ns/channel, using a LeCroy 2256-AS Waveform Digitizer. One advantage to this technique is that the PMT gain can be adjusted to prevent saturation when examining the larger bursts.

In one series of experiments the RE bursts were also digitized at 100 ns/channel so that the maximum amplitude of each burst could be measured.

The data from the RE and phE signals were stored in a LeCroy 3500 Data Acquisition System. All of the experiments were conducted in room air at 1 atmosphere of pressure unless otherwise specified.

3 RESULTS

3.1 Time correlations

When the adhesive is peeled from the release-coated polyester backing (substrate) copious phE and RE are observed. In Figure 2 we show simultaneous phE and RE measurements. The emission occurring in the first 10 s of the plots was for a peel speed of 35 mm/s. Qualitatively, the emission increased at the onset of

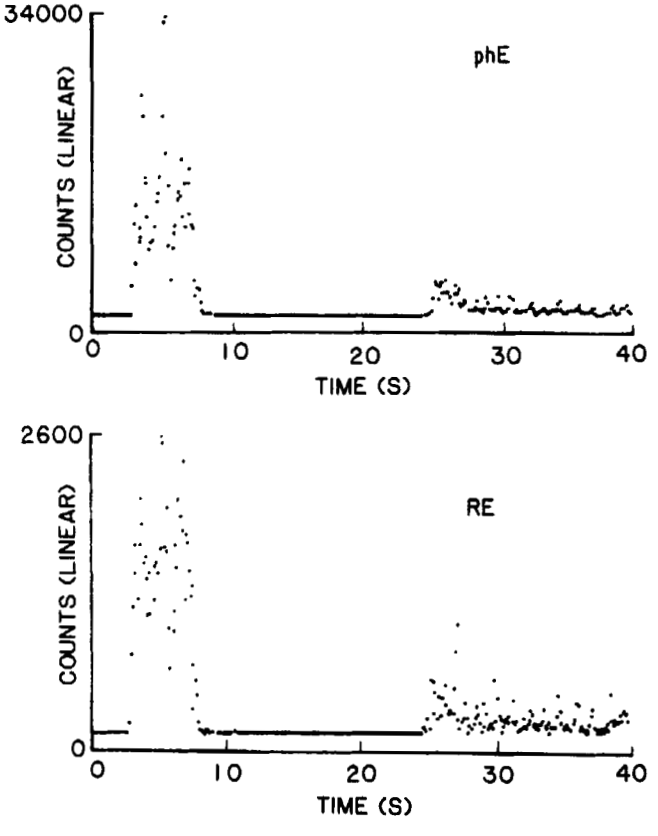

FIGURE 2 phE and RE counts *vs* time measured simultaneously for fast peeling (35 mm/s) and slow peeling (5 mm/s). Each point represents counts accumulated in a multichannel scaler for 0.12 s.

peeling and decreased rapidly when peeling was stopped. However, careful examination showed that emission continued *after* the displacement of the ends of the specimen was stopped, principally from additional peeling due to relaxation of the tape.

The emission rising at approximately 25 s on the plots in Figure 2 was for a second peel at a slower speed (5 mm/s). This shows the strong dependence of phE and RE intensity on the rate of separation of the adhesive from the substrate. This effect is similar to what we observed earlier in the phE for the same system and for interply delamination in Kevlar–Epoxy composites.[8] In general, the largest maxima in the phE and RE shown in Figure 2 appear to occur simultaneously.

In Figure 3, we compare on the same plot the decay of the photons and RE after the displacement was stopped (shown by the arrow). The RE curve shown as a solid line is a fit to the data. The phE that remains after the RE falls is a real "after-glow" and is seen to last on the order of seconds. It should be mentioned that if ones eyes are dark adapted, both the phE during peeling and the "after-glow" can be easily seen.

Figure 4 shows RE and phE measurements on a faster time scale (0.01 s/channel). We find "*oscillations*" in both the RE and phE rates, which rise and fall simultaneously. This irregular character in Figure 4 corresponds to the patchwise failure of the adhesive in an

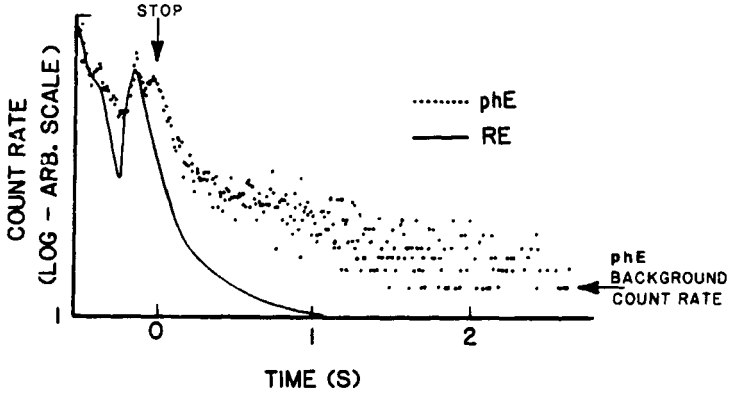

FIGURE 3 Decay of phE and RE signals when fast peel (shown in Figure 2) was stopped. The phE after the RE has fallen is due to an "after-glow".

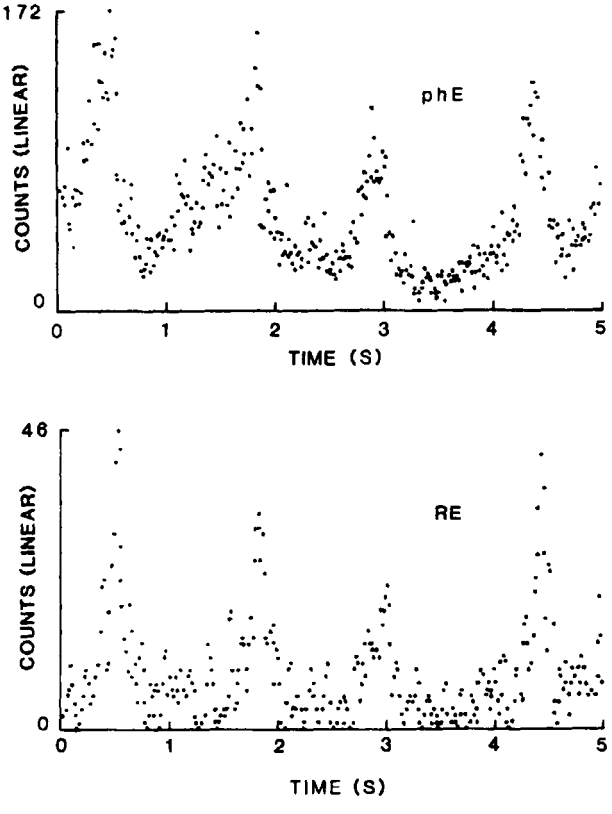

FIGURE 4 phE and RE counts *vs* time acquired at 0.01 s/channel.

oscillating or low peel rate "stick-slip" mode,[18,19] an effect which is accentuated by the presence of the fibers and stiffness of the adhesive. The peaks in the emission correspond to "slip" and the valleys correspond to "stick".

Upon examination of this emission on yet a faster time scale, one finds that emission such as seen in Figures 2 and 4 actually consist of a superposition of many faster RE and phE bursts. In order to prevent pile-up of these bursts, we conducted experiments at much slower peeling speeds (1–2 mm/s).

In Figure 5 we show typical photon bursts measured at 100 μs/channel. We note that bursts of photons appear to rise in a single

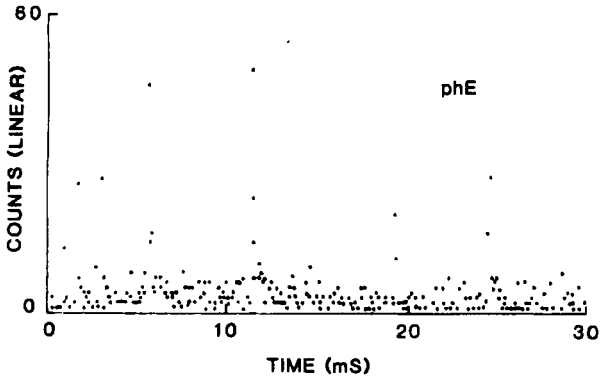

FIGURE 5 phE counts *vs* time acquired at 100 μs/channel.

channel and decay in times of approximately 150 μs. Although not evident here, we were able to show that the majority of these bursts were *saturating* our detector electronics so that in fact they are often considerably larger.

Time correlations between these RE and phE could be investigated using standard coincidence electronics. However, due to the relatively long duration of both the ringing signals from the RE and the phE decay, one would only learn that the two types of bursts were accompanying one another. Instead, we chose to trigger the multichannel scaler with a pulse near the onset of the RE burst and count the accompanying photons. If indeed the two bursts occur "simultaneously" one should observe a peak at or near the RE trigger. In this experiment, the data was accumulated at 1 μs/channel and the process repeated for a number of RE trigger pulses where each phE burst is added on top of the preceding bursts. The results are snown in Figure 6, indicating, indeed, a correlation between the RE and phE bursts.

We also see that there is a characteristic time distribution of phE accompanying the RE bursts. the problem with the data in Figure 6 is that the rise in intensity from $t = 0$, or perhaps better put, the depression of the intensity near $t = 0$, is an artifact of the very high photon counting rates accompanying and immediately following the RE trigger, again due to the saturation of the phE detector electronics. At approximately 10 μs after the trigger pulse the electronics recovers; the points beyond this time represent the

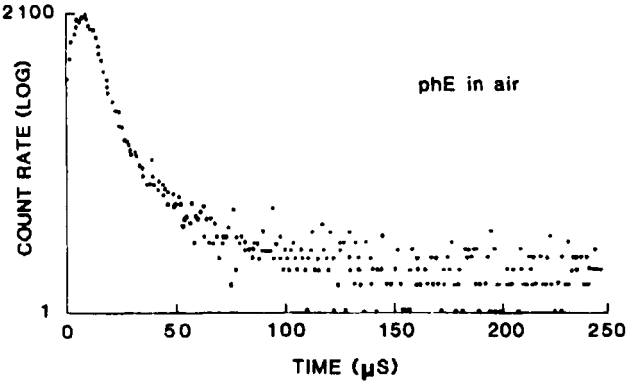

FIGURE 6 A correlation in time of the RE and phE. At $t = 0$, each RE trigger pulse started the multichannel scaler counting phE at 1 μs/channel.

actual decay in the photon count rate relative to the RE burst on the time scale of several μs. We suggest that this curve eventually blends into the tail shown in Figure 3. At this point it is not clear whether one single kinetics law could be used to fit this decay curve over such a wide range of times; we note here that the curve in Figure 6 is non-linear on a log scale and will comment further on these results in a later section.

An improved phE time distribution was obtained by treating the signal in an analog rather than digital mode, using a fast amplifier and a digitizer as described above. The RE trigger served as a convenient stop pulse for the digitizer. The digitized current from a single phE burst is shown in Figure 7, obtained at 50 ns/channel. As before, we repeatedly ran into saturation problems during the first few channels of the burst. On occasion, we would obtain a small unsaturated phE burst which showed only the initial part of the emission (200–300 ns wide, rising in 50 ns or less). By matching the "tail" of this emission with the curve of Figure 7 we are able to obtain a "composite" time distribution for the first 50 μs of the burst, which is shown in Figure 8 (note log scale). The important observation is that the initial spike is extremely intense relative to what is the *beginning* of a much lower intensity decay. Judging from the data of Figure 6, this decay lasts for several hundred μs and, in

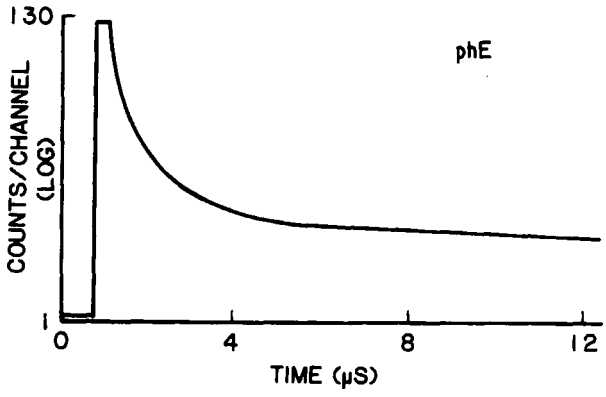

FIGURE 7 A single phE burst digitized at 50 ns/channel. Note saturation of the signal during the most intense interval (1 μs).

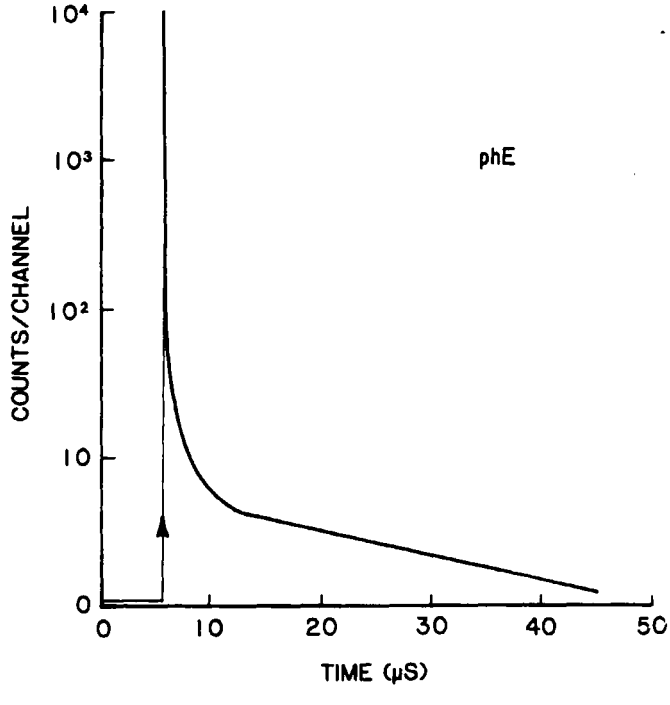

FIGURE 8 Composite phE curve using data of Figure 7 with digitized data from a single, unsaturated phE burst.

fact, in Figure 3, the collective "tail" of a large number of bursts can be seen to last for seconds.

The position of the RE trigger pulse can be accurately determined with respect to the onset of the front of the phE burst. These were in coincidence to within 100 ns, which was within the uncertainty of determining the start of the RE burst. Thus, to within this time interval, the RE burst and the intense part of the phE burst are occurring simultaneously.

By increasing the time constant of the amplifier (which basically adds some integration to the shape of the signal) we were able to measure the area of an unsaturated burst and calculate the number of photons contained in the bursts. For the larger phE peaks (taking into account the detector efficiency of 10^{-2}), we determine that typically 300 to 400,000 photons are entering the photon detector for each burst. This corresponds to peak counting rates exceeded 10^{10} photons/s. Unfortunately, we do not know the angular distribution of the phE so that it is difficult to estimate the actual total emission (we need the ratio of photons detected to the total which is given by the integral of the phE angular distribution over the solid angle subtended by the detector divided by the integral of the angular distribution over a sphere). However, assuming isotropic emission, we are detecting only approximately 4% of the total emission.

3.2 Correlation between the amplitude of RE bursts and photon intensity

A correlation in the amplitudes of the RE and phE bursts was determined in the following way. Each RE burst was digitized and its amplitude was measured. The simultaneous current pulse from the PMT was amplified (with sufficient time constant to capture the major portion of the emission) and digitized. The area, which is directly proportional to the number of photons released, was then measured. One set of data is shown in Figure 9 which resulted from the peeling apart of two layers of filament tape, (*i.e.*, assembled with their adhesive sides together.) We note two distinct and divergent groups of data points which were fit separately using a linear least squares method. The resulting fits, shown in Figure 9 as solid lines, had very different slopes yet each exhibited a correlation

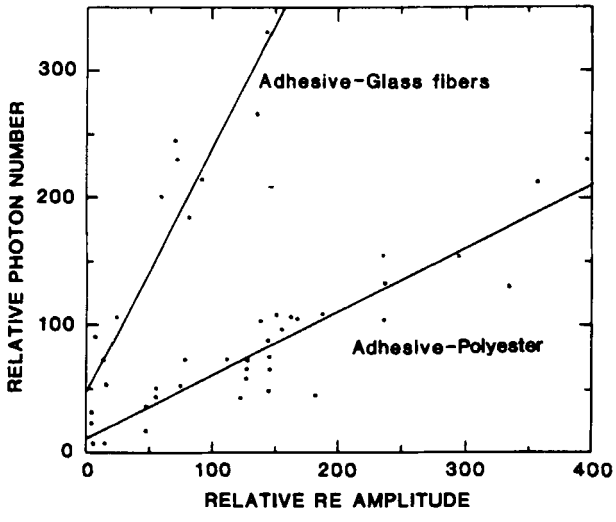

FIGURE 9 Correlation of the amplitudes of simultaneous RE-phE bursts. Solid lines are linear least squares fits to the two "clusters" of data.

coefficient of 0.94, implying a high probability of independent and linear behavior.

When we found two sets of data points in the results for this single experiment, we suspected that there were really two kinds of interfacial failure occurring during the test: the failure of the adhesive-glass filament interface and the failure of the adhesive-polyester interface. Other experiments confirmed this fact. By applying glass beads between the layers of adhesive we caused more failure to occur at the adhesive-glass bead interface. (This interface proved to be a very copious source of photons relative to the RE—resulting in a large slope of phE *vs* RE). We also delaminated the front adhesive + filament layer from the back adhesive + polyester layer and found that the back adhesive was dramatically different from the front adhesive in that the phE *vs* RE slope was also very large. Thus, the type of interface which is undergoing failure determines the characteristic slope of the phE *vs* RE amplitude curve.

It should be mentioned that we also observed a strong positive correlation between the intensity and duration of the decaying part of the phE with the RE intensity. Thus, the excitations necessary to

produce the "after-emission" were strongly influenced by the intensity of the discharge.

3.3 The role of the gaseous environment

The intense phE which occurred simultaneously with the RE resulted from photons produced during the discharges. We conjectured that the delayed phE might result from particle bombardment of the surfaces followed by a relaxation process which would be a form of phosphorescence. An alternative mechanism for this sustained phE is chemiluminescence. Fanter and Levy's discussion of the role of oxygen in the production of strain-induced phE from polymers[20] suggested to us that a chemiluminescence mechanism would be enhanced by the presence of oxygen. To determine if the decays observed after each discharge were due to a reaction with oxygen, we performed peeling experiments in O_2, N_2, and He at one atmosphere and room temperature. Data for these gases taken under the same peeling conditions (2 mm/s) and accumulation time as Figure 6 (performed in air) are shown in Figure 10.

When a comparison is made between Figures 10 and 6 the following is noted.

A. The later parts of all curves are qualitatively similar. Each gas displays a slowly varying phE with approximately the same decay kinetics.

B. The position of the early broad peak first observed in air is shifted. For the series of gases O_2, He, Air, and N_2 the peak appears at 1, 5, 8, and 25 μs respectively. This is due to *progressively higher initial phE signals* which produce progressively longer amplifier saturation.

C. We may calculate the average number of photons per RE burst for the series of gases O_2, Air, He, and N_2; this ratio was 21, 100, 126, and 144, respectively.

The result A shows that chemiluminescence involving oxygen is playing no detectable role in the delayed phE. The results B and C agree with the earlier comments concerning the saturation of the amplifier-discriminator at the highest photon counting intensity. In comparison with air the N_2 produces 40% more photons at each discharge. Thus the phE/RE ratio is greater and the counting is impeded in N_2 for 25 μs on average. In comparison with air, O_2

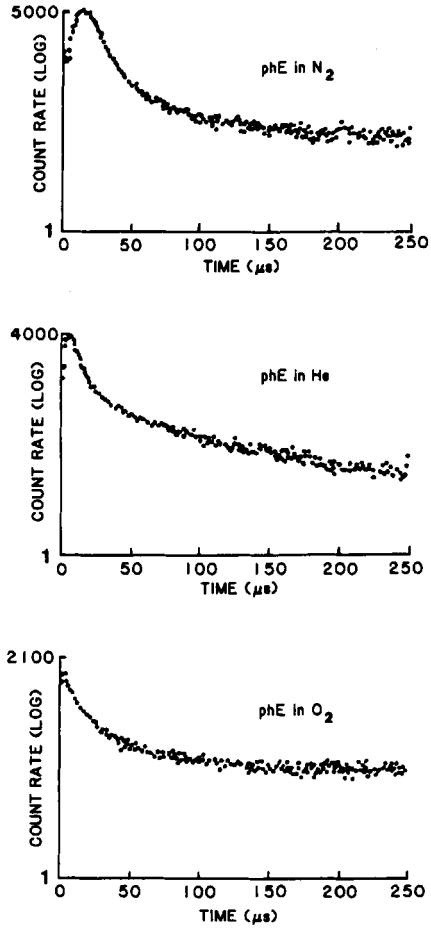

FIGURE 10 Accumulated RE-phE correlation curves taken in one atmosphere of N_2, He, O_2, respectively. Same conditions and accumulation time as Figure 6 which was taken in air.

produces about one-fifth as many photons at each discharge and allows the counter to function after one microsecond. The results for He are intermediate and He appears to support discharges that are slightly more emissive than those in air.

These results are consistent with the electrical breakdown properties of these gases. Oxygen has a fairly high electron affinity and

can readily form O^- and O_2^- and perhaps O_3^- and O_4^- when free electrons are present.[21,22] This attachment tends to remove electrons from a discharge before electrons gain sufficient energy to produce additional ion pairs by collision.[23] Thus, this attachment will reduce the intensity of the discharges and therefore reduce the amount of phE accompanying each discharge.

Neither He nor N_2 form negative ions by electron attachment so that they do not quench the avalanche process. N_2 seems to support a particularly emissive discharge. Mambetov and Masuraliev reported[24] some time ago that the phE from the adhesive failure at the interfaces of natural rubber with aluminum and glass was stronger in He than in air.

We next made a comparison of the RE for the two gases with most disparate properties toward discharge, O_2 and N_2. In order to make this comparison we measured the total number of RE bursts and the size distribution of RE in N_2 and in O_2 under the same peeling conditions (2 mm/s) and accumulation time. The results are shown in Figure 11. As expected, the N_2 yielded many more bursts

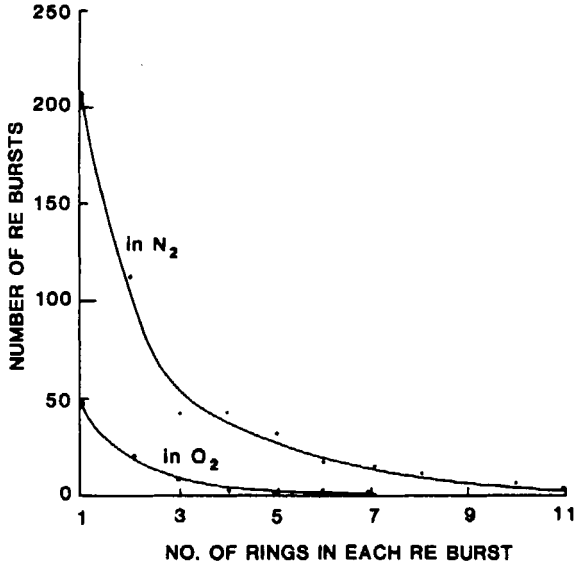

FIGURE 11 Comparison of total number and relative size of RE bursts in N_2 and O_2. Peeling speed 2 mm/s or 0.36 cm^2/s. For this experiment we detect 333 RE bursts/cm^2 of tape peeled in N_2 and 54 RE bursts/cm^2 in O_2.

and larger bursts than the O_2. For the same new surface area produced, the N_2 atmosphere resulted in the detection of over six times as many bursts as in O_2. On the average, the N_2 RE bursts displayed 1.5 times as many rings or oscillations as the bursts in O_2, indicating considerably larger amplitude RE bursts. The microdischarges are thus more energetic and would produce larger numbers of photons per accompanying RE burst, in agreement with C above.

This fact explains the larger ratio of photons per RE burst for N_2 as opposed to the other gases. We know that there is a positive size correlation between number of phE and the RE burst amplitude. RE bursts which are larger in size should be accompanied by more photons and yield a larger ratio of phE/RE in N_2, precisely the results described in C above. The results of this experiment also allowed us to calculate that on the average in N_2 one RE burst was detected for each 0.3 mm^2 of sample peeled.

4 DISCUSSION AND CONCLUSION

We interpret these results as follows: Intense charge separation on the fracture surfaces produced by adhesive failure leads to micro-discharges in the region of the crack tip. These micro-discharges are responsible for the production of electromagnetic bursts (RE). These bursts are accompanied by "spikes" of phE which are extremely rapid and have decay times of less than 50 ns. The peak phE count rate can exceed 10^{10} photons/s. The onset of phE and RE are in coincidence to within 100 ns and correlate in size in a manner that is unique to *where* the failure has occurred.

During the breakdown event the freshly created surfaces will be exposed to the products of the discharge (charged particles, perhaps UV radiation). This bombardment can have two effects: It can cause the immediate release of more charged particles which enhances the discharge process; and it can cause excitation of the surfaces so that delayed emission can occur. When polymers are stimulated with energetic radiation thermally stimulated processes can lead to photon emission (thermal luminescence). When this occurs immediately after formation of the necessary excitations, it is referred to as phosphorescence. The intensity and duration of the resulting phosphorescence will depend on the "dose" the polymer

surface received during the discharge.[25] Thus we conclude that the sustained emission we observe is indeed due to the relaxation of an excited fracture surface, where the surface excitation came from the discharge. In relatively low resolution spectra taken of light accompanying adhesive failure of other adhesive-substrate materials, Ohara *et al.*[26] and Klyueva *et al.*[27] have seen evidence of both gaseous and luminescence-like emission. It would be particularly interesting to do time-resolved-spectroscopy to separate the fast and slow components. The latter should be pure luminescence.

To the extent that the *intensity of the discharge* is influenced by the gaseous environment, we have the observed differences in the intensities for the different gases; *i.e.*, N_2 yielded the strongest emission and O_2 the weakest emission. Furthermore, once the discharge and bombardment of the surfaces were complete, the shape of the delayed decay curves were independent of the gas and only differed in magnitude depending on the intensity of the discharge. This implies first that the decay kinetics are thus a property of the *polymer*, and second the "after-glow" is not induced by chemiluminescence from a reaction involving oxygen.

If we peel in a particular gas (*e.g.*, air), we find that other factors can influence the number and size of the RE and phE bursts, *e.g.*, the peel speed. The major effect here is most likely the details of the charge separation process. The faster one separates the two dissimilar materials, the less likely reneutralization can occur by motion of charge. This leads to higher charge densities and therefore stronger electic fields and more intense discharges. Furthermore, when the separation rate is modulated in time by the "stick-slip" phenomena, corresponding fluctuations result in varying charge densities and discharge intensities. These variations in discharge intensities then lead to corresponding changes in the phE and RE intensities. Current studies on imaging the phE bursts are showing dramatic and extremely sensitive responses to near microscopic features of the mechanics of adhesive failure.

A second factor that influences the net charge separation and resulting emission is variation of the substrate. Thus if different interfaces are involved (adhesive-glass *vs* adhesive-polyester), for example, we observe a proportionality constant between the magnitudes of RE and phE which is characteristic of the particular interface and may uniquely signify the locus of each individual microscopic failure event.

Finally, we note that a number of the RE and phE characteristics should be similar to the behavior of electron and positive ion emission which are necessarily observed in vacuum. Our major goal is to continue measuring the characteristics of these emissions, determine in more detail the mechanisms, and identify the dependences of fractoemission on the details of failure.

Acknowledgments

We wish to thank L. C. Jensen, Washington State University, for his assistance in these experiments.

This work was supported by McDonnell Douglas Independent Development Fund, the Office of Naval Research Power Program under Contract N00014-80-C-0213, NR 659-803, and NASA-Ames Interchange NCA2-OR840-202.

References

1. B. V. Deryagin, N. A. Krotova, and V. P. Smilga, *Adhesion of Solids,* (English Translation) (Consultants Bureau, New York, 1978).
2. J. Wollbrandt, E. Linke, and K. Meyer, *phys. stat. sol.* (*a*) **27,** K53–K55 (1975).
3. J. T. Dickinson, D. B. Snyder, and E. E. Donaldson, *J. Vac. Sci. Tech.* **17,** 429 (1980).
4. J. T. Dickinson, E. E. Donaldson, and M. K. Park, *J. Mat. Sci.* **16,** 2897 (1981).
5. J. T. Dickinson, M. K. Park, E. E. Donaldson, and L. C. Jensen, *J. Vac. Sci. and Technol.* **20,** 436 (1982).
6. M. H. Miles and J. T. Dickinson, *Appl. Phys. Lett.* **41,** 924 (1982).
7. J. T. Dickinson, L. C. Jensen, and M. K. Park, *Appl. Phys. Lett.* **41,** 827 (1982).
8. J. T. Dickinson, *Fracto-Emission Accompanying Adhesive Failure,* in *Adhesive Chemistry—Developments and Trends,* L. H. Lee, Ed. (Plenum Publishers, New York, 1984).
9. J. T. Dickinson, A. Jahan-Latibari, and L. C. Jensen, *Fracto-Emission from Fiber-Reinforced and Particulate Filled Composites,* in *Polymer Composites and Interfaces,* N. G. Kumar and H. Ishida, Eds. (Plenum Publishers, New York, 1985).
10. J. T. Dickinson, L. C. Jensen, and A. Jahan-Latibari, *Rubber Chem. Tech.* **56,** 927 (1983).
11. J. T. Dickinson, L. C. Jensen, and A. Jahan-Latibari, *J. Vac. Sci. Technol.* **A2,** 1112 (1984).
12. J. T. Dickinson, L. B. Brix, and L. C. Jensen, *J. Phys. Chem.* **88,** 1698 (1984).
13. J. T. Dickinson, A. Jahan-Latibari, and L. C. Jensen, *J. Mat. Sci.* **20,** 229 (1985).
14. J. T. Dickinson and L. C. Jensen, *J. Poly. Sci.: Poly. Phys. Ed.,* in press.
15. B. V. Deryagin, L. A. Tyurikova, N. A. Krotova, and Y. P. Toporov, *IEEE Trans. Indust. Appl.* Vl. **IA-14,** 541 (1978).
16. S. M. Skinner, *J. Appl. Phys.* **26,** 498 (1955).
17. J. R. Huntsberger, *The Mechanisms of Adhesion,* in *Treatise on Adhesion and Adhesives,* Vol. 1, R. L. Patrick, Ed. (Marcel Dekker, New York, 1967).
18. D. Satas, *Handbook of Pressure-Sensitive Adhesive Technology,* Chapter 4, D. Satas, Ed. (Van Nostrand Reinhold Co., New York, 1982).

19. A. J. Duke, *J. Appl. Polym. Sci.* **18,** 3019 (1974).
20. D. L. Fanter and R. L. Levy, ACS Symposium Series No. 95: *Durability of Macromolecular Materials,* R. K. Eby, Ed. 211 (1979).
21. B. M. Smirnov, *Negative Ions* (McGraw-Hill Inc., Newark, NJ, 1982).
22. H. S. W. Massie, *Negative Ions,* 3rd. Edition (Cambridge Univ. Press, 1976).
23. A. Von Engel, *Ionozed Gases,* 2nd. Edition (Clarendon Press, Oxford, 1965), p. 186.
24. D. M. Mambetov and T. Masuraliev, *Doklad. Akad. Nauk SSSR* **185,** 122 (1964).
25. R. Chen and Y. Kirsh, *Analysis of Thermally Stimulated Processes* (Pergamon Press, 1981), pp. 18–22.
26. K. Ohara and T. Hata, *J. Appl. Polym. Sci.* **14,** 2079 (1970).
27. V. A. Klyueva, *et al. Colloid Journal* (*Kolloidn. Zh.*) **41,** 287 (1979).